Biochimie xxx (2013) 1–10

Contents lists available at SciVerse ScienceDirect

Biochimie

journal homepage: www.elsevier.com/locate/biochi

Research paper

Membrane cholesterol and sphingomyelin, and ostreolysin A are obligatory for pore-formation by a MACPF/CDC-like pore-forming protein, pleurotolysin B

Katja Ota [a], Adrijana Leonardi [b], Miha Mikelj [a], Matej Skočaj [a], Therese Wohlschlager [c], Markus Künzler [c], Markus Aebi [c], Mojca Narat [d], Igor Križaj [b,e,f], Gregor Anderluh [a,g], Kristina Sepčić [a], Peter Maček [a,*]

[a] Department of Biology, Biotechnical Faculty, University of Ljubljana, Večna pot 111, SI-1000 Ljubljana, Slovenia
[b] Jožef Stefan Institute, SI-1000 Ljubljana, Slovenia
[c] Department of Biology, Institute of Microbiology, ETH Zürich, Zürich, Switzerland
[d] Department of Animal Science, Biotechnical Faculty, University of Ljubljana, SI-1230 Domžale, Slovenia
[e] Centre of Excellence for Integrated Approaches in Chemistry and Biology of Proteins, SI-1000 Ljubljana, Slovenia
[f] Department of Chemistry and Biochemistry, Faculty of Chemistry and Chemical Technology, University of Ljubljana, SI-1000 Ljubljana, Slovenia
[g] National Institute of Chemistry, SI-1000 Ljubljana, Slovenia

ARTICLE INFO

Article history:
Received 14 February 2013
Accepted 12 June 2013
Available online xxx

Keywords:
Aegerolysin
Cholesterol-dependent cytolysin
Lipid-binding protein
Membrane attack complex
Pleurotolysin
Pleurotus ostreatus

ABSTRACT

The mushroom *Pleurotus ostreatus* has been reported to produce the hemolytic proteins ostreolysin (OlyA), pleurotolysin A (PlyA) and pleurotolysin B (PlyB). The present study of the native and recombinant proteins dissects out their lipid-binding characteristics and their roles in lipid binding and membrane permeabilization. Using lipid-binding studies, permeabilization of erythrocytes, large unilamellar vesicles of various lipid compositions, and electron microscopy, we show that OlyA, a PlyA homolog, preferentially binds to membranes rich in sterol and sphingomyelin, but it does not permeabilize them. The N-terminally truncated Δ48PlyB corresponds to the mature and active form of native PlyB, and it has a membrane attack complex-perforin (MACPF) domain. Δ48PlyB spontaneously oligomerizes in solution, and binds weakly to various lipid membranes but is not able to perforate them. However, binding of Δ48PlyB to the cholesterol and sphingomyelin membranes, and consequently, their permeabilization is dramatically promoted in the presence of OlyA. On these membranes, Δ48PlyB and OlyA form predominantly 13-meric oligomers. These are rosette-like structures with a thickness of ~9 nm from the membrane surface, with 19.7 nm and 4.9 nm outer and inner diameters, respectively. When present on opposing vesicle membranes, these oligomers can dimerize and thus promote aggregation of vesicles. Based on the structural and functional characteristics of Δ48PlyB, we suggest that it shares some features with MACPF/cholesterol-dependent cytolysin (CDC) proteins. OlyA is obligatory for the Δ48PlyB permeabilization of membranes rich in cholesterol and sphingomyelin.

1. Introduction

The white-rot fungus *Pleurotus ostreatus* is a non-pathogenic wood-decaying basidiomycetous species. Like other *Pleurotus* spp., this is a massively cultivated mushroom worldwide as it is considered safe for human and animal nutrition, and to provide medical benefits. It also serves in biotechnological and environmental applications, which exploit its high potential for degradation of ligno-cellulose materials [1].

Basidiocarps of *P. ostreatus* were originally reported to contain pleurotolysin, a cytolytic, ~12-kDa protein that is inhibited by sphingomyelin [2]. A ~15-kDa cytolytic protein belonging to the

Abbreviations: CDC, cholesterol-dependent cytolysin; H_6-OlyA6, N-terminally hexa-histidine-tagged OlyA6; H_6-Δ48PlyB, N-terminally hexa-histidine-tagged N-truncated precursor of PlyB (Acc. code AB177872, lacking 48 amino acids at N-terminus); OlyA6, ostreolysin A6; OlyA6-H_6, C-terminally hexa-histidine tagged OlyA6; nOlyA, native ostreolysin A; nPlyB, native pleurotolysin B; POPC, 1-palmitoyl-2-oleoyl-*sn*-glycero-3-phosphocholine.

* Corresponding author. Tel.: +386 1 3203395; fax: +386 1 2573390.
E-mail address: peter.macek@bf.uni-lj.si (P. Maček).

0300-9084/$ – see front matter © 2013 Elsevier Masson SAS. All rights reserved.
http://dx.doi.org/10.1016/j.biochi.2013.06.012

aegerolysins (reviewed in Ref. [3]) and known as ostreolysin (Oly) was later isolated from *P. ostreatus* [4,5]. However, it was reported by Tomita et al. [6] that a *P. ostreatus* protein, the native 15-kDa pleurotolysin A (PlyA) that is very similar to ostreolysin, is not hemolytic unless supplemented with another mushroom protein, ~59-kDa pleurotolysin B (PlyB). Neither PlyA nor PlyB were hemolytic *per se*, even at up to 100 μg/mL [6,7]. Another difference reported for Oly and PlyA is their lipid-binding selectivity. In contrast to Oly, PlyA and PlyB have been reported to form a sphingomyelin-dependent binary cytolysin [6]. Other aegerolysin-like proteins that have been reported to be cytolytic include eryngeolysin from *Pleurotus eryngii* [8] and Asp-hemolysin from *Aspergillus fumigatus* [9]. In contrast to Oly and PlyA, Asp-hemolysin and a non-cytolytic aegerolysin, PA0122, from the bacterium *Pseudomonas aeruginosa* have been shown to interact with oxidized low-density lipoprotein (LDL) and with lysophosphatides [10–12]. However, most of the aegerolysins (Pfam06355) have not been functionally characterized neither is understood their biological role. These 15–17 kDa proteins are distributed among bacteria, fungi, plants, and were also found in one insect and viral species. They are characterized biochemically as all-β structured proteins with low isoelectric points and stability in a wide pH range [3].

There have been ambiguous reports on the cytolytic and lipid-binding characteristics of aegerolysins and PlyB. PlyB contains a predicted membrane attack complex-perforin (MACPF) domain [13,14], which is typical of MACPF/cholesterol-dependent cytolysin (CDC) pore-forming proteins [15]. Similarities in the three-dimensional (3D) structures of PlyB and the MACPF/CDC proteins stimulated us to reinvestigate the hemolytic activity of the native proteins purified *de novo*. This included investigating the binding and membrane-permeabilizing properties of a recombinant ostreolysin isoform, named OlyA6 (95% identity with PlyA), and of the N-terminally truncated precursor of PlyB (Δ48PlyB). Δ48PlyB corresponds to the purified mature form of the native PlyB (475 amino acids) that has been reported to be much more hemolytic than the recombinant full-length precursor of PlyB (523 amino acids) [6,7].

We clarify here that the observed hemolytic activity of the native ~15-kDa ostreolysin, isolated previously [4], was due to incomplete separation from the native PlyB. We show that OlyA6 interacts exclusively with membranes rich in cholesterol and sphingomyelin. However, OlyA6 does not permeabilize these membranes, although it induces significant changes in the shape of these lipid vesicles. In solution, OlyA6 is monomeric, and does not interact with Δ48PlyB. Although Δ48PlyB forms SDS-resistant oligomers *per se* in solution and in the presence of vesicle membranes, we confirm that Δ48PlyB cannot efficiently bind to and lyse red blood cells and cholesterol-rich cholesterol/sphingomyelin vesicles without assistance of the native OlyA or recombinant OlyA6 variants. As seen with electron microscopy (EM), Δ48PlyB oligomers are ring-like structures while the 13-meric rosette-like structures are formed on the vesicles by Δ48PlyB in the presence of OlyA6. In agreement with their cholesterol/sphingomyelin preference, Δ48PlyB and OlyA6 are non-toxic to *Arabidopsis thaliana* and only weakly toxic to *Caenorhabditis elegans*; i.e. organisms that do not synthesize sphingomyelin or sterols, respectively. Since the biological role of these proteins is completely unknown the data presented herein may provide some clues for further studies.

2. Materials and methods

2.1. Reagents and materials

The FastDigest® restriction enzymes *Bam*HI, *Mlu*I, *Nde*I, *Xho*I, and rapid DNA ligation kits, GeneJET™ PCR purification kits, GeneJET™ Gel extraction kits, Transformaid™ bacterial transformation kits, GeneJET™ plasmid miniprep kits, and PageRuler™ prestained protein ladder were all from Fermentas. The pET plasmids were from Novagen. Oligonucleotide primers and the gene coding for Δ48PlyB, the N-truncated form of PlyB (GI: 54312023, accession number AB177870.1), were synthesized by MWG Operon. Biacore SPR chips were from GE Healthcare. Murine anti-penta-histidine antibodies were from Qiagen (Germany), and secondary goat anti-mouse IgG-horse radish peroxidase antibodies were from Santa Cruz Biotechnology. Sphingomyelin (porcine brain), cholesterol, 1-palmitoyl-2-oleoyl-*sn*-glycero-3-phosphocholine (POPC), and 1-palmitoyl-2-hydroxy-*sn*-glycero-3-phosphocholine (16:0) (lysophosphatidylcholine) were from Avanti Polar Lipids (USA). Total lipids from bovine erythrocyte membranes were extracted using a Bligh and Dyer method [16], as described previously [17]. All lipids were stored under nitrogen at −80 °C.

Protein concentrations were determined using the Pierce BCA protein assay reagents (Thermo Scientific). Protein size and purity were analyzed using SDS-PAGE, with homogenous 10% or 12% acrylamide gels. The proteins were stained with silver or Coomassie blue. When transferred to PVDF membranes (Millipore, USA) for Western blotting, the proteins were detected with anti-penta-histidine antibodies (Qiagen, Germany) or anti-Oly antibodies, when appropriate. Thrombin was from Novagen (USA). Other materials and analytical grade chemicals were from Sigma–Aldrich and Merck. MonoQ and PD-10 desalting columns were purchased from GE Healthcare (USA), and Amicon® Ultra-4 centrifugal filter units were from Millipore (USA).

2.2. Preparation of native and recombinant OlyA and PlyB

Native OlyA (nOlyA) and PlyB (nPlyB) were purified from *P. ostreatus* (Plo5 strain) using a modified procedure of Berne et al. [4] (see Supplementary material).

An OlyA6 clone from a cDNA library prepared from the total mRNA of *P. ostreatus* (strain Plo5 from the ZIM collection of the Biotechnical Faculty, University of Ljubljana, Slovenia) [5] was used to construct the recombinant OlyA variants. The genes coding for OlyA6 and Δ48PlyB were cloned into the pET8c vector using the *Bam*HI and *Mlu*I sites, and the pET21c(+) vector using the *Nde*I and *Xho*I sites. This provided expression constructs with or without C-terminal or N-terminal hexahistidine (H_6) tags, a thrombin cleavage site (LVPR), and linkers. Nucleotide sequences were determined by MWG Operon. The oligonucleotide sequences and the protein designations and their relative molecular masses are presented in Supplementary material (Table S1) and Fig. 1, respectively.

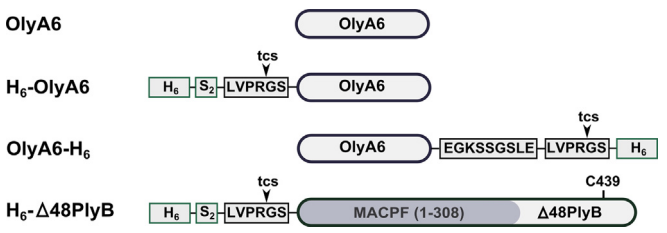

Fig. 1. Domain structure and tags of the OlyA6 and Δ48PlyB proteins investigated in this study. OlyA6, ostreolysin A6; H_6-OlyA6, N-terminally hexa-histidine tagged OlyA6; OlyA6-H_6, C-terminally hexa-histidine-tagged OlyA6; H_6-Δ48PlyB, N-terminally hexa-histidine-tagged N-truncated PlyB (Acc. code AB177872, without 48 amino acids at the N-terminus); H_6, hexa-histidine; S_2, di-serine and EGKSSGSGLE, peptide linkers; tcs, thrombin cleavage site; C439, single cysteine 439. Calculated relative molecular masses, M_r: OlyA6, 14,961.6; H_6-OlyA6, 16,699.5; GS-OlyA6, 15,236.9; OlyA6-H_6, 17,326.1; OlyA6-LVPR, 15,427.2; Δ48PlyB, 52,078.6; H_6-Δ48PlyB, 53,685.3; GS-Δ48PlyB, 52,222.7. For nOlyA, the M_r of 14,854 was taken from Ref. [5].

Please cite this article in press as: K. Ota, et al., Membrane cholesterol and sphingomyelin, and ostreolysin A are obligatory for pore-formation by a MACPF/CDC-like pore-forming protein, pleurotolysin B, Biochimie (2013), http://dx.doi.org/10.1016/j.biochi.2013.06.012

The OlyA6 and Δ48PlyB variants were expressed in the BL21(DE3) *Escherichia coli* strain, and purified as detailed in Supplementary material. When appropriate, the H_6 tag was removed with thrombin (Novagen, EMD4 Biosciences, EMD Millipore, USA) using 1 U/mg thrombin at 22 °C for 16 h. Prior to this thrombin cleavage, the Ni^{2+}-NTA elution buffer was exchanged for thrombin cleavage buffer (20 mM Tris–HCl, 150 mM NaCl, 2.5 mM $CaCl_2$, pH 8.4) on a PD-10 desalting column (GE Healthcare, USA). After cleavage, the sample buffer was exchanged for 20 mM Tris–HCl, pH 8.0, and used in further purification on a MonoQ anion-exchange column. The protein was eluted with a 0–100 mM NaCl gradient in the same buffer. Isolation of the non-tagged variant, OlyA6, required the MonoQ re-chromatography.

The Δ48PlyB proteins were expressed insoluble in inclusion bodies and the active proteins were seen to be refolded, as described in Supplementary material. The purified proteins (yield, ~1 mg/L culture) were aliquoted and stored in 140 mM NaCl, 20 mM Tris–HCl, 5% (v/v) glycerol, pH 8.0, at −80 °C. Freshly thawed aliquots were used in the functional studies, to minimize spontaneous protein degradation.

2.3. Mass spectrometry and LC–MS/MS amino-acid sequencing

The nOlyA isoforms and nPlyB were analyzed using a 1200 series HPLC-Chip-LC/MSD Trap XCT Ultra mass spectrometer (Agilent Technologies, Germany) and a MALDI-TOF/TOF UltrafleXtreme III mass spectrometer (Bruker, USA). Prior the LC–MS/MS analysis, the MonoQ-purified nOlyA peak was separated on a C_4-reverse-phase HPLC column using a 0–90% acetonitrile gradient in 0.1% (v/v) trifluoroacetic acid, and digested with proteomics grade trypsin (Sigma, USA). The Econo HighS fraction containing nPlyB was separated by SDS-PAGE on 12.5% (w/v) polyacrylamide gels. The Coomassie blue stained protein band at ~59 kDa was excised and destained in a siliconized tube. The protein in the gel was then reduced with dithiothreitol, alkylated with iodoacetamide, and digested overnight with trypsin. The resulting peptides were extracted from the gel in 50% (v/v) acetonitrile/5% (v/v) formic acid, and concentrated for LC–MS/MS analysis. Mass spectrometry data were analyzed using the Spectrum Mill software Rev A.03.03.084 SR4 (Agilent Technologies, Santa Clara, CA, USA) on the National Center for Biotechnology Information (NCBI) protein database, and the Joint Genome Institute (JGI) raw genome data (*P. ostreatus* PC15 v2.0) [18].

2.4. Preparation of large unilamellar vesicles

Lipids extracted from bovine erythrocytes, and mixtures of cholesterol:sphingomyelin 1:1 or 1:4 (mol/mol ratio), or cholesterol:POPC 1:1, or POPC were dissolved in $CHCl_3$:MeOH (3:1, v/v) at ~10 mg/mL. Large unilamellar vesicles (LUVs) of ~100-nm diameter were prepared in 20 mM Tris–HCl, 140 mM NaCl, 1 mM EDTA, pH 8.0 (vesicle buffer) at room temperature, by extruding multilamellar vesicles through a 0.1-μm polycarbonate filter (Millipore) mounted in a small-volume extruder (Avestin, Canada), as described previously [17,19]. The cholesterol and choline-lipid content of the LUVs was determined using cholesterol C and phospholipid Lab-Assay™ kits, respectively. For calcein-loaded LUVs, 60 mM calcein in water (MQ-grade) was used instead of vesicle buffer. Extra-vesicular calcein was removed by gel filtration on a 0.7 cm × 7 cm Sephadex G-50 column, which was eluted with vesicle buffer. These LUVs were stored at 4 °C and used within 2 days.

2.5. Hemolytic assay

Hemolytic activity was measured on a kinetic microplate reader (MRX, Dynex) at ~25 °C, as described previously [20]. The density of the bovine erythrocyte suspension in 140 mM NaCl, 20 mM Tris–HCl, pH 7.4 (erythrocyte buffer) was adjusted to an apparent absorbance at 630 nm (A_{630}) of 0.5. After the addition of the serially diluted proteins, the decrease in A_{630} was measured for 30 min at 7 s intervals, to determine the t_{50}, as the time necessary for 50% hemolysis. The hemolytic activities are expressed as $1/t_{50}$ (min^{-1}).

2.6. Calcein release from LUVs

Permeabilization of calcein-loaded LUVs of various lipid compositions (see Preparation of large unilamellar vesicles) was assayed in a fluorescence microplate reader (Fluostar, SLT, Austria) at ~25 °C. The calcein-loaded LUVs (synthetic lipid, 40 μM) in vesicle buffer and the protein sample (1:1, v/v) were sequentially dispensed into a multi-well microplate. The erythrocyte lipid LUV concentration was adjusted to give a comparable maximal fluorescence response. The LUVs were excited at 485 nm and the intensity of the emitted light (F) of released (de-quenched) calcein at 538 nm was monitored at 30 s intervals for 30 min. The intensity of the emitted light at $t = 0$ min was designated as F_0. The LUVs were finally lysed with 1 mM Triton X-100, to determine the maximal fluorescence intensity, F_{max}, which corresponded to 100% calcein release. The percentage of calcein release, R (%), was then determined as:

$$R(\%) = \frac{F - F_0}{F_{max} - F_0} * 100 \quad (1)$$

2.7. Analysis of the interactions of proteins with membrane components

The binding of OlyA6-H_6 and/or H_6-Δ48PlyB to erythrocyte membranes was monitored using Western blotting, and the interaction of OlyA6-LVPR with carbohydrates was assayed on a Consortium for Functional Glycomics (CFG) printed glycan array [21], as described in Supplementary material.

Formation of SDS-resistant protein oligomers was detected by SDS-PAGE using precast 4–12% NuPAGE® Novex Bis-Tris gels. OlyA6-LVPR and H6-Δ48PlyB, either alone or combined, were incubated without or with cholesterol:sphingomyelin (1:1, mol/mol) LUVs in 20 mM Tris–HCl, 140 mM NaCl, 1 mM EDTA, pH 8.0, at various protein/protein and lipid/protein molar ratios. After incubation on a Thermo Shaker at 400 rpm at 25 °C for 2 h, the samples were analyzed by SDS-PAGE and silver staining. The optical densities of the bands were analyzed using ImageJ.

2.8. Surface plasmon resonance measurements

The kinetics of the interactions were monitored on BiacoreX and Biacore T100 surface plasmon resonance (SPR)-based refractometers, and the data were processed with BIAevaluation software (GE Healthcare). Binding of proteins to lipid membranes was determined using LUVs of various lipid compositions and lipid molar ratios (see Preparation of large unilamellar vesicles). The LUVs were prepared and captured on an L1 sensor chip, and the experiments were run as described previously [22,23] (for details, see Supplementary material).

We also studied the interactions of immobilized OlyA6-LVPR, with OlyA6-LVPR, H_6-Δ48PlyB, lysophosphatidylcholine, and the detergent SDS as analytes. OlyA6-LVPR was coupled to a CM5 chip at up to 120 RU using the standard N-hydroxysuccinimide/N-ethyl-N′-[3-dimethyl aminopropyl]-carbodiimide coupling procedure recommended by the manufacturer. For protein–protein

Please cite this article in press as: K. Ota, et al., Membrane cholesterol and sphingomyelin, and ostreolysin A are obligatory for pore-formation by a MACPF/CDC-like pore-forming protein, pleurotolysin B, Biochimie (2013), http://dx.doi.org/10.1016/j.biochi.2013.06.012

interactions, two different concentrations of OlyA6-LVPR or H_6-Δ48PlyB (5 μM, 20 μM) were injected over the chip, as for lysophosphatidylcholine (4 μM, 400 μM) and SDS (1 mM, 10 mM). The samples were injected at a flow rate of 30 μL/min for 60 s, in phosphate buffered saline (20 mM Na_2HPO_4/NaH_2PO_4, 140 mM NaCl, pH 7.4) as the running buffer. Sensorgrams were corrected for the untreated surface flow-cell response.

2.9. Electron microscopy

Erythrocyte lipid LUVs or cholesterol:sphingomyelin 1:1 LUVs were incubated with the proteins in 140 mM NaCl, 20 mM Tris–HCl, 1 mM EDTA, pH 8.0, at room temperature. A 4 μL sample was left for 60 s on a carbon-grid that had been previously glow-discharged for 30 s, and excess solution was removed with Whatman filter paper. To reduce salt effects, three droplets of deionized water were adhered to the grid for 1–2 s. After removal of the excess fluid, the grid was negatively stained with 2% (w/v) uranyl acetate for 30 s, with the excess staining solution blotted and the grid allowed to dry. The specimens were examined with a Tecnai Spirit electron microscope operated at 80 kV. The data were collected at a magnification of 48,000×, with a 4000 × 4000 FEI Falcon CCD camera. EM images were processed with EMAN2 [24].

3. Results

3.1. Modeling of 3D structures

Modeling of the 3D structure and the 3D alignment predicted PlyB as a MACPF/CDC-type protein, with the highest similarity to mouse perforin (PDB: 3NSJ) with regard to the MACPF domain. The homology modeling predicted a β-sandwich fold for OlyA6, the 3D structure to be most similar to that of sea anemone fragaceatoxin C (PDB: 3LIM) (see Supplementary material, Fig. S1).

3.2. Native and recombinant proteins

Separation of the ammonium-sulfate-precipitated proteins is shown in Fig. S2 (Supplementary material). SDS-PAGE of the MonoQ P3.1 and P3.2 fractions indicated the presence of two proteins (Fig. S2D) with an apparent molecular mass of ~17 kDa, and with both hemolytically active only when combined with purified nPlyB or recombinant Δ48PlyB variants. Further analysis revealed the presence of an ~25-kDa contaminant in P3.1; therefore, we used the P3.2 fractions as the source of purified nOlyA in further experiments. C_4-reverse-phase HPLC of nOlyA demonstrated two separate isoforms, designated nOlyA1 and nOlyA2, that are highly homologous to the recombinant variant OlyA6 and PlyA [6], as confirmed by LC-MS/MS sequencing (Supplementary material, Fig. S3). In contrast to nOlyA, the final yield of nPlyB, which showed an apparent molecular mass of ~60 kDa and was located in the Econo HighS P2.2 fraction, was much lower and contained some impurities (Supplementary material, Fig. S2F). The presence of nPlyB was confirmed by LC-MS/MS sequencing (40% coverage with PlyB; NCBI acc. number BAD66667.1). As nPlyB was unstable and degraded during storage the recombinant variant Δ48PlyB, which corresponds to the mature form of nPlyB [6,7], was used exclusively in the functional studies.

We prepared and characterized recombinant protein variants of OlyA6 and Δ48PlyB, and their thrombin-cleaved derivatives (see Fig. 1 for structures and nomenclature, and Fig. S4 for SDS-PAGE analysis). The relative molecular masses (M_r) of H_6-OlyA6 and OlyA6-H_6 were determined using MALDI-TOF MS, and were 17,327.6 and 16,700.0, respectively. These values are in good agreement with the calculated M_r. As with nPlyB, H_6-Δ48PlyB and GS-Δ48PlyB were prone to spontaneous degradation in solution. The preparation of H_6-Δ48PlyB for MALDI-TOF MS (concentration, buffer change, reverse-phase HPLC), for example, resulted in its almost complete degradation into several fragments. The M_r could be determined for only two of these (17,743.7, 17,758.7). The dissolved proteins were more stable when kept frozen in buffers containing 5% (v/v) glycerol. It is of note that, in contrast to C-terminal tags, N-terminal tags completely prevented the binding of the recombinant OlyA6 variants to lipids (Fig. 4B), and as such, these proteins did not promote hemolysis when combined with the Δ48PlyB variants (Fig. 2A) It is not clear whether this was due to improper folding or whether the tags obstructed the binding of the protein to the lipid surface. In most functional studies we used C-terminally tagged OlyA6 variants with or without the hexahistidine tag due to their easy purification. The Δ48PlyB variants, although their hemolytic activities were not identical, were functional in combination with functional OlyA variants.

3.3. Membrane permeabilization and binding studies

The purified native and recombinant proteins, both individually and combined, were initially assayed for hemolytic activity with bovine red blood cells. Typically, a sigmoidal time-course of hemolysis was observed, as reported previously [4,17]. All of the OlyA proteins were not hemolytic *per se*, even at ≥10 μM, unless combined with H_6-Δ48PlyB or its thrombin-cleaved form. The potency of the OlyA proteins to promote H_6-Δ48PlyB-induced hemolysis

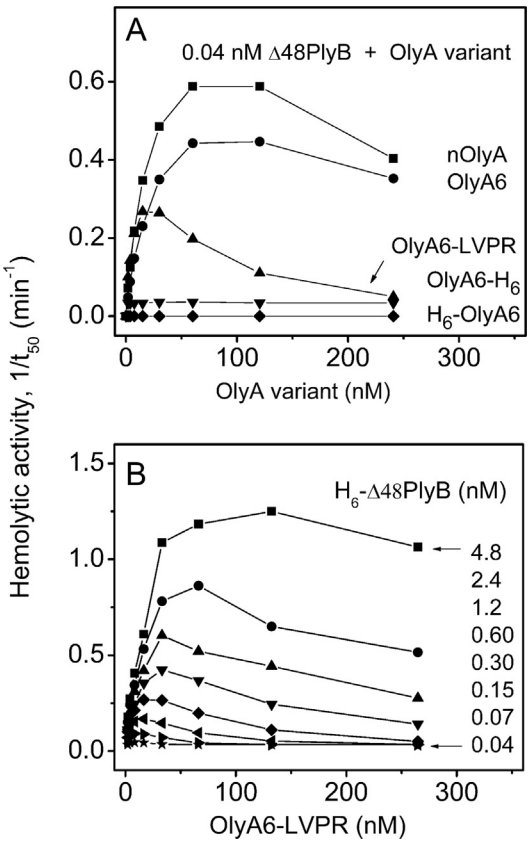

Fig. 2. Hemolytic activity of H_6-Δ48PlyB in combination with OlyA variants. Time courses of hemolysis (as $1/t_{50}$) were monitored with a microplate reader at 630 nm, to determine time to 50% hemolysis, t_{50}. (A) Hemolytic activity of 2.4 nM H_6-Δ48PlyB supplemented with native (nOly) and recombinant OlyA6 proteins. (B) Dependence of hemolytic activity of H_6-Δ48PlyB on OlyA6-LVPR concentration. Inset numbers indicate nM H_6-Δ48PlyB.

Please cite this article in press as: K. Ota, et al., Membrane cholesterol and sphingomyelin, and ostreolysin A are obligatory for pore-formation by a MACPF/CDC-like pore-forming protein, pleurotolysin B, Biochimie (2013), http://dx.doi.org/10.1016/j.biochi.2013.06.012

decreased in the order of: nOlyA > OlyA6 > OlyA6-LVPR > OlyA6-H_6, while H_6-OlyA6 and its thrombin-cleaved derivative completely lacked any effect (Fig. 2A). Although less effective in these hemolytic assays than the OlyA6 variant, OlyA6-LVPR was mostly used in further experiments for two reasons: (i) its preparation was rather easy by using conventional Ni^{2+}-NTA chromatography, and (ii) in preliminary experiments OlyA6-LVPR exhibited qualitatively the same mode of action as nOly or recombinant OlyA6.

The hemolytic activity was dependent on the concentrations of both of the proteins, as illustrated in Fig. 2B for the H_6-Δ48PlyB plus OlyA6-LVPR mixture. The apparent inhibition of hemolysis at increasing concentrations of nOlyA or its recombinant variants with constant H_6-Δ48PlyB is shown in Fig. 2.

We also tested the permeabilizing activity of these proteins on calcein-loaded LUVs with various lipid compositions. In addition to being hemolytic, H_6-Δ48PlyB combined with the OlyA variants also released encapsulated calcein from the erythrocyte lipid LUVs in a concentration-dependent manner, as illustrated in Fig. 3A for the combination of H_6-Δ48PlyB plus OlyA6-LVPR. With regard to the lipid composition of the LUVs, this permeabilizing activity of these combined proteins was greater for LUVs prepared from the erythrocyte total lipid extract, lower for cholesterol:sphingomyelin 1:1, poorly detected for cholesterol:sphingomyelin 1: 4, and not seen for cholesterol:POPC 1:4 (Fig. 3B) and POPC LUVs (data not shown).

Western blotting showed that OlyA6-H_6 alone readily binds to the erythrocyte membranes, while the binding of H_6-Δ48PlyB alone was minimal, and was detected only when greater amounts of membranes with bound H_6-Δ48PlyB were analyzed. However, when these proteins were combined, OlyA6-H_6 bound to a similar extent as seen without H_6-Δ48PlyB, while this significantly stimulated the binding of H_6-Δ48PlyB to the membranes (see Supplementary material, Fig. S5).

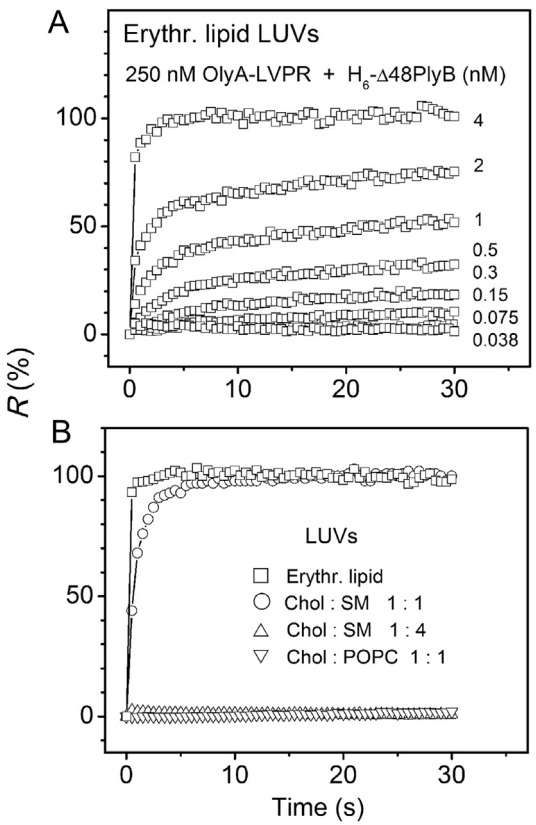

Fig. 3. Permeabilization of LUVs of various lipid compositions, with combined H_6-Δ48PlyB and OlyA6-LVRP. Fluorescence intensity of calcein released from LUVs of various lipid compositions as indicated prepared in 20 mM Tris–HCl, 140 mM NaCl, 1 mM EDTA, pH 8.0, monitored as described in Experimental procedures. (A) Permeabilization of LUVs made of total erythrocyte lipids by 250 nM OlyA6-LVPR and H_6-Δ48PlyB at various nM concentrations as indicated. (B) Effect of 150 nM H_6-Δ48PlyB combined with 250 nM OlyA6-LVPR on the permeabilization of LUVs of various lipid compositions, as indicated.

SPR studies of the interactions of these proteins with on-chip immobilized LUVs provided additional data on the avidity of these proteins for membrane lipids, as shown in Fig. 4. The difference in the binding properties of GS-Δ48PlyB with the LUVs as compared to the OlyA proteins was remarkable (Fig. 4B, C). Consistently with the hemolysis results we found nOly and the non-tagged OlyA6 variant most effective in the lipid binding. The C-terminal tags obviously decreased avidity for the tested lipids; as longer the tag slower was lipid binding. In contrast to nOlyA and the non-tagged or C-terminally tagged OlyA, GS-Δ48PlyB showed a lower affinity and less selectivity for the lipids tested. As shown in Fig. 4A, B, the binding of 1–4 μM GS-Δ48PlyB to the erythrocyte lipid LUVs resulted in 25 RU to 100 RU, while for 1.0 μM of the OlyA proteins (except those that were N-terminally tagged), the response reached was more than 4000 RU. This difference between the proteins was the lowest with the cholesterol:sphingomyelin 1:1 LUVs (Fig. 4C, D). In contrast to OlyA, GS-Δ48PlyB bound to all of the LUVs tested (Fig. 4D), while OlyA bound only to the erythrocyte lipid LUVs and the cholesterol:sphingomyelin 1:1 LUVs (Fig. 4B, D). The OlyA proteins, except those that were N-terminally tagged, markedly promoted the binding of both variants of Δ48PlyB in the case of the erythrocyte lipids, and less so with cholesterol:-sphingomyelin 1:1, but not with the other LUVs (e.g., see nOlyA and GS-Δ48PlyB in Fig. 4D). None of the association–dissociation kinetics traces could be fitted to the kinetics models provided by the BIAevaluation package.

In the SPR study of the interactions of immobilized OlyA-LVPR, there was no binding with OlyA-LVPR, H_6-Δ48PlyB or lysophosphatidylcholine as analytes, while the SDS control bound weakly and reversibly (data not shown). These results suggest that OlyA6-LVPR, and so most likely other OlyA variants, does not oligomerize spontaneously in solution neither it interacts with H_6-Δ48PlyB without assistance of lipids. The screening for OlyA6-LVPR binding to an array of 611 human glycans also showed no significant interactions (data not shown).

As has been seen for several pore-forming proteins, H_6-Δ48PlyB can form SDS-resistant oligomers in solution, which can be enhanced by the cholesterol:sphingomyelin 1:1 LUVs, as shown in Fig. 5. OlyA6-LVPR alone did not result in protein aggregates, regardless of the presence of the LUVs (Fig. 5A, B). In contrast, with H_6-Δ48PlyB either alone or in combination with OlyA6-LVPR in solution, there were regularly formed SDS-resistant oligomers with molecular masses greater than 433 kDa. Two or three sizes of oligomer can be seen in the SDS-PAGE analysis shown in Fig. 5B. The band density of these oligomers positively correlated with the amounts of each of the lipids and of OlyA6-LVPR. Of note, the higher density of oligomer bands corresponded to the consumption of monomeric H_6-Δ48PlyB. Moreover, Western-blot analysis of SDS-resistant oligomers by using anti-OlyA6 and anti-H_6-Δ48PlyB monoclonal antibodies revealed the presence of H_6-Δ48PlyB but not OlyA6 in the oligomers (Supplementary material, Fig. S6).

3.4. Electron microscopy

The EM images of the erythrocyte lipid LUVs and the cholesterol:sphingomyelin 1:1 LUVs exposed to $OlyA_6$-LVPR and/or H_6-Δ48PlyB were very similar. Erythrocyte lipid LUVs treated with $OlyA_6$-LVPR and/or H_6-Δ48PlyB are shown in Fig. 6. $OlyA_6$-LVPR alone induced a marked change of the LUV shape, as seen in Fig. 6A.

Please cite this article in press as: K. Ota, et al., Membrane cholesterol and sphingomyelin, and ostreolysin A are obligatory for pore-formation by a MACPF/CDC-like pore-forming protein, pleurotolysin B, Biochimie (2013), http://dx.doi.org/10.1016/j.biochi.2013.06.012

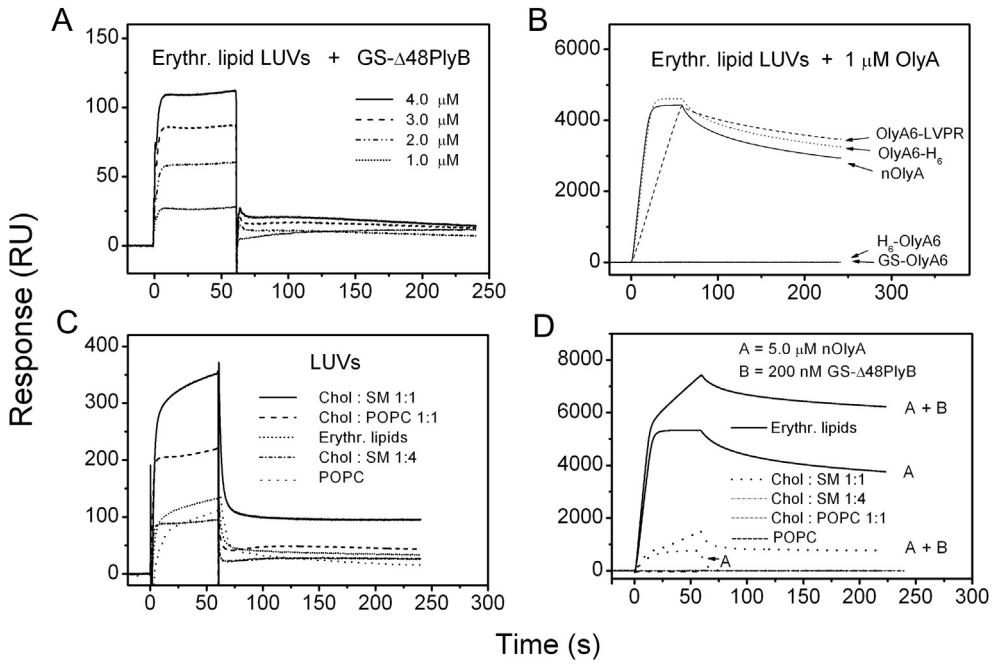

Fig. 4. SPR analysis of the interactions of Δ48PlyB and the OlyA variants with LUVs. Vesicles were immobilized on a Biacore L1 chip to 10,000 ± 1000 RU and analytes injected at a flow rate of 10 μL/min in running buffer (140 mM NaCl, 20 mM Tris–HCl, 1 mM EDTA, pH 8.0) at 25 °C. Representative sensorgrams of triplicates are shown. (A) Association-desorption kinetics of GS-Δ48PlyB at the indicated concentrations. (B) Sensorgrams for 1 μM OlyA variants binding to erythrocyte lipid LUVs. (C) Effect of various lipid compositions of LUVs on the association-desorption kinetics of 4.0 μM GS-Δ48PlyB. (D) nOlyA (5.0 μM), either alone (A) or mixed with 200 nM GS-Δ48PlyB (A + B), was injected over LUVs of varied lipid composition.

Membrane ruffling and budding resulted in various LUV shapes, and even vesicle scission was seen. These effects of $OlyA_6$-LVPR alone were much less pronounced, or not seen, when these LUVs were exposed to the $OlyA_6$-LVPR plus H_6-Δ48PlyB mixture. In contrast to $OlyA_6$-LVPR alone, H_6-Δ48PlyB alone (Fig. 6B) did not result in changes in the vesicle shapes, but with two types of oligomers seen: ring-like and rosette-like structures in solution, and rosette-like structures on the vesicle membranes. The dimensions of these membrane-attached H_6-Δ48PlyB rosettes were 19.8 ± 0.5 nm in diameter, with a thickness of 9.2 ± 0.2 nm from the membrane surface (means ± s.d.; $n = 6$). When the proteins were combined, no ring-like oligomers were seen, although the number of rosette-like structures was markedly increased on the LUVs (Fig. 6C). On these LUV membranes, the dense packing of these structures resulted in a hexagonal array, as shown in Fig. 6C (bottom panel). When combined with $OlyA_6$-LVPR, H_6-Δ48PlyB produced significant aggregation of the LUVs. Inspection of these LUV aggregates revealed that the rosette-like structures can associate in a top-surface to top-surface manner, to form dimeric rosette-like structures that can thus connect opposing LUV membranes (see Fig. 6C, top panel, and Fig. 6D, right panel). Image averaging of the dominating rosette-like oligomers produced by the combined $OlyA_6$-LVPR plus H_6-Δ48PlyB proteins (Fig. 6D, left panel) revealed a 13-meric structure with ~19.7 nm in outer diameter, and with a central circle of diameter ~4.9 nm with a higher density. The thickness of these single rosette-like oligomers was ~9 nm, as can be seen in the side-view of the dimeric structure in Fig. 6D (right panel).

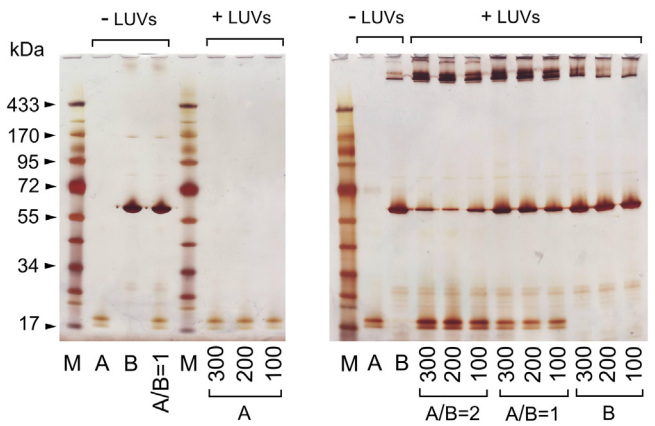

Fig. 5. Formation of SDS-resistant oligomers in solution and with the cholesterol:sphingomyelin 1:1 LUVs. Representative experiments for H_6-Δ48PlyB (B), at a constant 4 μM, and OlyA6-LVPR (A), alone or combined, were incubated without (−LUVs) or with cholesterol:sphingomyelin 1:1 LUVs (+LUVs) in 20 mM Tris–HCl, 140 mM NaCl, 1 mM EDTA, pH 8.0, at varied lipid/protein molar ratios (300, 200, 100), and protein/protein ratios (A/B), and analyzed on silver-stained 4–12% SDS-PAGE gels (see Experimental procedures). *M*, molecular mass markers (kDa; as indicated).

4. Discussion

Our investigation here of the cytolytic properties of these native and recombinant OlyA and PlyB variants provides evidence that the smaller OlyA protein alone does not permeabilize erythrocyte or LUV membranes. This has already been reported for the OlyA close homologs of pleurotolysin A from *P. ostreatus* [6,7] and erylysin A from *P. eryngii* [25]. Thus, the previously reported cytolytic activity of Oly (and most likely also of aegerolysin from *Agrocybe aegerita*) [4] can be ascribed to its incomplete separation from PlyB. As shown here and by Tomita et al. [6], the presence of ≤1 nM PlyB renders a mixture with OlyA (or its homolog) hemolytic. Moreover, the modified purification of the native proteins used here shows that *P. ostreatus* produces several isoforms of nOlyA, two of which have been partially sequenced. This is in agreement with reports

Please cite this article in press as: K. Ota, et al., Membrane cholesterol and sphingomyelin, and ostreolysin A are obligatory for pore-formation by a MACPF/CDC-like pore-forming protein, pleurotolysin B, Biochimie (2013), http://dx.doi.org/10.1016/j.biochi.2013.06.012

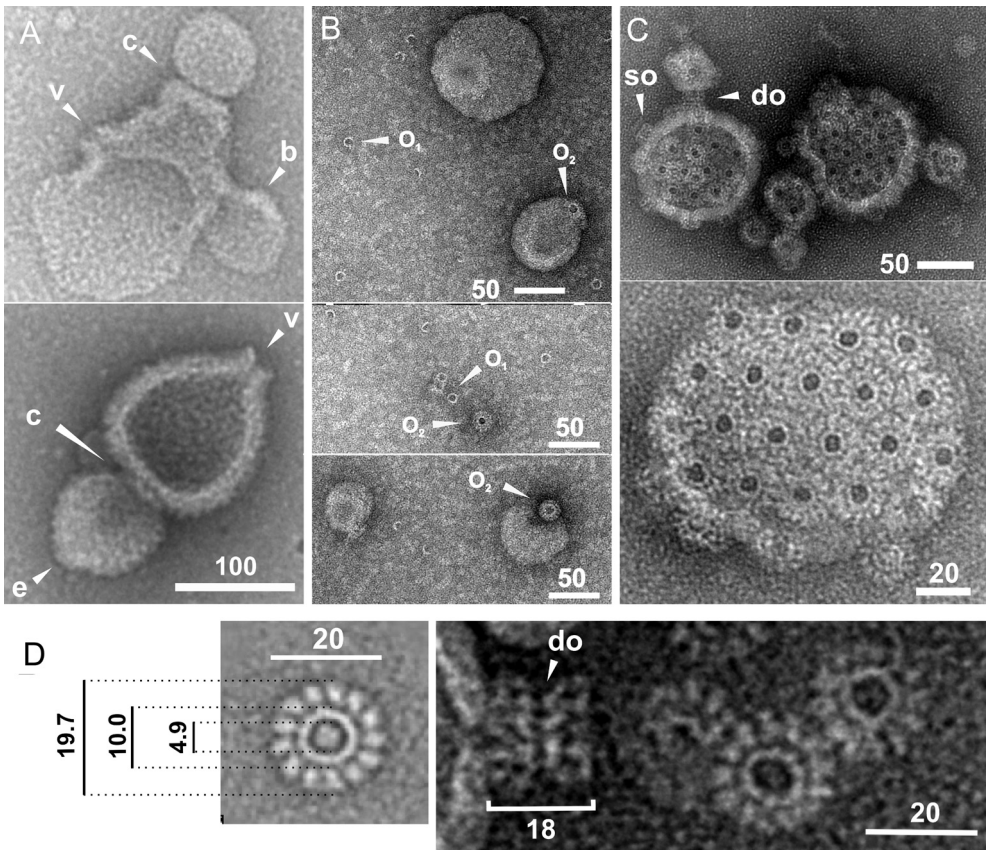

Fig. 6. Representative EM images of erythrocyte lipid LUVs treated with OlyA6-LVPR and H_6-Δ48PlyB. OlyA6-LVPR and H_6-Δ48PlyB, individually or combined, were incubated with LUVs in 140 mM NaCl, 20 mM Tris–HCl, 1 mM EDTA, pH 8.0, and transferred to carbon EM grids, with 2% uranyl acetate for contrast. Scale bars given in nm. (A) LUVs treated with 4 μM OlyA6-LVPR. b, vesicle budding; c, vesicle constriction; e, evagination; v, "volcano-like" structure. (B) LUVs treated with 4 μM H_6-Δ48PlyB; o_1, ring-like structures, o_2, rosette-like structures. (C) Top: LUVs treated with the combination of 533 nM OlyA6-LVPR and 266 nM H_6-Δ48PlyB; do, dimeric rosette-like oligomer, so, single rosette-like oligomer. Bottom: Single LUV treated with the combination of 8 μM OlyA6-LVPR and 4 μM H_6-Δ48PlyB, showing hexagonal array of rosette-like oligomers obtained. (D) Left: Averaged image ($n = 9$) of a 13-meric rosette-like oligomer formed on LUVs treated with OlyA6-LVPR and H_6-Δ48PlyB. Right: Detail of dimeric rosette-like oligomers (do), ~18 nm in height, connecting two opposing LUV membranes (see also C). Bars and numbers indicate dimensions in nm.

that some fungi can synthesize numerous mRNAs that encode various aegerolysin isoforms [26,27].

Our SPR studies reveal that in contrast to Asp-hemolysin and the *P. aeruginosa* protein PA0122 [10–12], OlyA does not interact with lysophosphatidylcholine. The interaction of PA0122 with lysophospholipids has been suggested to have a pleiotropic function; i.e., a modulatory role in microbial film formation and host innate immunity [19]. However, it appears that the properties and biological roles of the aegerolysins are diverse and are dependent on their organism of origin, as is also the case for the MACPF/CDC proteins [14]. In organisms reported or predicted to produce both aegerolysins and PlyB orthologs (i.e., *Aspergillus chrysogenum*, *Aspergillus flavus*, *Penicillium chrysogenum*, *Neosartorya fischeri*, *P. ostreatus*, *P. eryngii*, *Agrocybe cylindracea*, *Trametes versicolor*, and *Heterobasidion annosum*), one of the possible roles of these aegerolysins might be the modulation of the activity of PlyB-like proteins.

Membrane permeabilization by Δ48PlyB is in line with its predicted 3D structural similarity to MACPF/CDC proteins [14,28]. The MACPF domain is crucial for the formation of transmembrane pores, through its restructuring of particular helices into hairpin β-strands, which then insert into the membrane lipid bilayer [14,28,29]. However, PlyB differs from perforin and CDCs in the C-terminal region. BLAST search reveals that the C-terminal amino acid sequence of Δ48PlyB is unique and clearly different from the perforin C2 domain [29] or the CDCs domain 4 [30] that enable lipid binding of these proteins. Only the single cysteine 439, which is proximal to the C-terminus of Δ48PlyB, may resemble the characteristics of CDCs [14,15,30–32] to some extent. The 3D similarity features also in the EM-imaged oligomeric structures of Δ48PlyB on the membranes. However, in contrast to other MACPF/CDCs that mostly use a higher number of monomers (>30), Δ48PlyB predominantly forms oligomers with 13-fold symmetry. Another difference is that in contrast to CDCs that require cholesterol for binding (excepted those that use a membrane protein receptor for attachment) and are partially inhibited by sphingomyelin [33], Δ48PlyB *per se* binds, although weakly and without membrane perforation, to the range of lipids assayed here, including to pure POPC, albeit that increased membrane cholesterol is preferred.

Previous experiments with partially purified ostreolysin [4] that will have containing minor amounts of PlyB, as discussed above, have revealed that the binding and membrane permeabilization are exclusively dependent on erythrocyte lipids, containing both cholesterol and sphingomyelin [34], and artificial sterol/sphingomyelin-rich membranes [17,35,36]. We have shown here that Δ48PlyB alone, although at relatively high concentrations, also interacts with LUVs that do not contain cholesterol; i.e., POPC LUVs. However, Δ48PlyB does not permeabilize these LUVs, even in the presence of the OlyA variants. Hence, it can be seen that the affinity of OlyA for the erythrocyte lipid LUVs and cholesterol:sphingomyelin LUVs dictates efficient membrane attachment of Δ48PlyB, and subsequently the efficient

Please cite this article in press as: K. Ota, et al., Membrane cholesterol and sphingomyelin, and ostreolysin A are obligatory for pore-formation by a MACPF/CDC-like pore-forming protein, pleurotolysin B, Biochimie (2013), http://dx.doi.org/10.1016/j.biochi.2013.06.012

permeabilization of these lipid membranes. This resembles the recruitment of the membrane attack complement component (MAC) C9 to targeted membranes [37,38]. The higher avidity of OlyA variants for the erythrocyte lipid LUVs as compared to the cholesterol:sphingomyelin LUVs might arise because of specific lipid microdomains inherent to the lipid composition of the erythrocyte membrane, which can include glycosphingolipids [39]. It is less likely that these erythrocyte glycosphingolipids serve directly as (co)acceptors, as binding of OlyA to mammalian glycans has not been shown. In line with the significance of the combination of a sterol and sphingomyelin for membrane binding of these proteins is the result of toxicity assays.

Another interesting feature of the cholesterol and sphingomyelin dependence of OlyA binding, which promotes the efficient binding of Δ48PlyB and the subsequent membrane permeabilization, is that the cholesterol needs to exceed a threshold of ≥30 mol %, as also seen previously with Oly [35]. This is also a property of the CDCs [30], such as, for example, perfringolysin [40] and listeriolysin [41]. These CDCs, however, do not require the supplement of sphingomyelin. Taken together, it appears that OlyA binds preferentially to membranes that are rich in sterol and sphingomyelin, as has been observed previously for the 'impure' Oly [35,36].

The pathways of pore-forming proteins from being in solution to the formation of the final transmembrane pore that involves the assembly of β-hairpins and/or α-helices can be diverse. Generally, one process might involve single molecules that attach to the membrane first, which can be followed by a downstream process of oligomerization, formation of the pre-pore, and finally the formation of the full transmembrane pore. Alternatively, oligomers might already be assembled in solution and then they can attach to the membrane to form a pre-pore that then rearranges to punch through the membrane [42]. Our data suggest that Δ48PlyB can already oligomerize to some extent in solution, forming SDS-resistant oligomers. This process is independent of the presence of OlyA. However, in the presence of the cholesterol:sphingomyelin 1:1 LUVs, the amount of SDS-resistant oligomers significantly increased. This is also in agreement with the appearance of the ring-like and rosette-like oligomers on the vesicles, as we have seen from our EM. In contrast, OlyA does not form SDS-resistant oligomers in solution or in the presence of lipids, but it does increase the amount of Δ48PlyB SDS-resistant oligomers in the presence of the LUVs, along with the number of rosette-like structures in the absence of SDS. At present, it is not clear whether these ring-like structures represent the pre-pore assembly, whereby the rosette-like structure represents the final pore. Ring-like structures rather than rosette-like oligomers have already been observed before on erythrocytes [6]. In contrast to this previous study [6] we cannot detect OlyA in SDS-resistant oligomers. We suggest that either our mix of three anti-OlyA monoclonal antibodies could not access binding epitopes when OlyA was included in the SDS-resistant oligomers or OlyA association with oligomerized PlyB was only loose, and thus broken upon the SDS treatment. Solving this ambiguity is in progress by the use of Ni^{2+}-NTA-Nanogold particles to label OlyA6-H_6 in the on-membrane rosette-like oligomers in order to be visualized with EM. Preliminary results (to be published elsewhere) confirmed the previous observation of Tomita et al. [6] who detected PlyA as a part of the SDS-resistant PlyB/PlyA oligomers by using polyclonal anti-PlyA antibodies.

Although there are some differences, the EM images of the rosette-like structures of the Δ48PlyB oligomers are like the circular pre-pore/pore structures formed by perfringolysin and pneumolysin on membranes [43,44]. An unprecedented peculiarity is, however, the top-surface to top-surface dimerization of the Δ48PlyB rosette-like oligomers on the membrane, which can thereby connect opposing membranes, to result in vesicle aggregation. Consistent with the number of monomers in the oligomers, the diameter of the perfringolysin pore that is formed by 32 monomers is 37 nm, while that of the most abundant 13-meric PlyB rosette is 19.7 nm. Similarly, the diameter of the 38-meric pneumolysin pore is 40 nm. The calculated width of a perfringolysin monomer in its pore is 2.44 nm, which is comparable to the 2.34 nm of Δ48PlyB. The dimensions of the monomers in the pore axial direction are also comparable, as seen by the thickness of the protein ring, which is 8 nm for perfringolysin, 8.5 nm for pneumolysin, and 7.9 nm for Δ48PlyB. The different numbers of monomers in these pore assemblies also results in an inner diameter of the pneumolysin pore of ~18 nm, while that of the Δ48PlyB rosette is ~4.9 nm. This value for the Δ48PlyB rosette is in good agreement with a previous estimation of a hydrodynamic (inner) diameter of ~4 nm for the Oly pores (which was contaminated with PlyB; see above) [17]. This dimeric rosette-like Δ48PlyB oligomer extends to a height of ~9 nm above the membrane, which is intermediate between the ~11.3 nm and 7.3 nm of the perfringolysin pre-pore and pore complex, respectively [45], or the 10 nm and 7 nm for pneumolysin, respectively [44].

The effects of OlyA on the susceptible membranes and its role in the recruitment of Δ48PlyB to membranes that we have seen here are intriguing. However, the present study does not provide enough evidence for any firm conclusions on an underlying molecular mechanism to be made. The EM images of the LUVs exposed to OlyA suggest that its binding evokes stress in the targeted membrane leaflet. This in turn leads to local changes in the membrane curvature, and consequently, to membrane bending and the appearance of various membrane and vesicle shapes. Of note, no such bending was observed with the combination of OlyA and Δ48PlyB, which suggests that when Δ48PlyB binds to and inserts into the membrane, this relaxes the OlyA-induced membrane stress. Proteins that bind to membranes can induce membrane remodeling that can result in membrane budding and blebbing, and even in the scission of vesicles [46,47]. This is dependent on the lipid composition, and on the presence of sterols in particular [48]. It is not clear whether such membrane remodeling by OlyA increases the affinity of Δ48PlyB for the membrane simply *via* changes in the membrane curvature, or whether the consequence of the membrane stress with OlyA induces the creation of specific lipid microdomains that are more susceptible to the insertion of Δ48PlyB. Furthermore, as discussed above, OlyA might recruit Δ48PlyB in a way that is similar to that observed for the MAC proteins. In this respect, it is interesting to note that the excess concentrations of OlyA suppress hemolytic activity, which implies that membrane curvature does not have a crucial role here. The inhibition was clearly dependent on the protein molar ratios. This suggests instead that the excess OlyA, which has a much higher affinity for the lipids than Δ48PlyB, can compete with Δ48PlyB for membrane binding sites. Such a tentative mechanistic scenario is also compatible with the observation that Δ48PlyB itself may assemble into SDS-resistant oligomers on membranes. However, the role of sterol/sphingomyelin-rich membrane domains in both protein binding and pore formation, along with the protein composition, remain to be elucidated.

The biological roles of PlyB and OlyA are not known. OlyA6-LVPR and H_6-Δ48PlyB had no effect on the germination and development of *A. thaliana* seedlings, while these proteins are only slightly toxic to *C. elegans*. This might correlate with the (co)occurrence of the OlyA and/or Δ48PlyB acceptors, and in particular with cholesterol, or other sterols, and sphingomyelin in these organisms. In contrast to vertebrates and plants, nematodes are sterol auxotrophs, and

Please cite this article in press as: K. Ota, et al., Membrane cholesterol and sphingomyelin, and ostreolysin A are obligatory for pore-formation by a MACPF/CDC-like pore-forming protein, pleurotolysin B, Biochimie (2013), http://dx.doi.org/10.1016/j.biochi.2013.06.012

they require dietary cholesterol or other sterols for reproduction, growth and development [49,50]. *C. elegans* acquires cholesterol from food supplies and accumulates it differentially along the intestine [43], while nematodes can produce sphingomyelin [51]. On the other hand, sphingomyelin is not typical for plants, which synthesize other membrane sphingolipids instead [52]. Assuming that the glycans are not the acceptors for OlyA, as seen on the CFG-glycan array, the weak toxicity of OlyA and PlyB in *C. elegans* might be because of the co-occurrence of dietary cholesterol and sphingomyelin in *C. elegans* but not in *A. thaliana*. However, we cannot exclude the possibility that the low toxicity results at least in part from the eventual decay of Δ48PlyB during the toxicity trial. It seems that rather having a defensive role PlyB and OlyA might play some other roles such as i.e. signaling, cell adhesion, or development as suggested for some other MACPF/CDC proteins [14,15,53]. Indeed, the mixture of nOly and nPlyB interacted with vesicles made of *P. ostreatus* total lipids, but did not permeabilize them [17]. This is therefore suggestive that the dimeric PlyB rosette-like structures can also be formed in the fungus.

5. Conclusions

We have provided evidence here that Δ48PlyB, which is predicted structurally to be a MACPF/CDC-like protein, may oligomerize in the presence of lipids, however, it permeabilizes very selectively cholesterol/sphingomyelin-rich membranes only if supplemented with OlyA. The poor and rather non-selective binding of Δ48PlyB to lipid membranes is dramatically stimulated by OlyA, a sterol/sphingomyelin-binding protein. The present study also clarifies that OlyA alone cannot permeabilize membranes as reported before [4] but appears to instead induce membrane stress that leads to considerable remodeling of the membrane. However, exact molecular mechanism of its assistance in the formation of transmembrane pores by Δ48PlyB remains to be elucidated. We have also shown for the first time that the 13-meric rosette-like assembly of Δ48PlyB is similar to the perfringolysin and pneumolysin pores. We suggest that the OlyA and PlyB proteins, not known to be secreted, have unknown intracellular roles, and that dimerization of the membrane-based Δ48PlyB oligomers represents a functional part of the role of Δ48PlyB.

Acknowledgments

This work was supported by the Slovenian Research Agency (grants P1-0207 and J1-4305). We are grateful to Ioan Iacovache from the Swiss Federal Institute of Technology, Lausanne, for EM experiments, image processing and critical reading of the manuscript. We thank Michelle Dunstone from the Monash University, Melbourne, for a generous gift of a PlyB sample and fruitful discussions. We acknowledge The Consortium for Functional Glycomics and the Protein–Carbohydrate Interaction Core H at the Emory University School of Medicine, Atlanta, GA, for glycan array analysis. We thank Dr. Marko Fonović and Robert Vidmar from the Department of Biochemistry and Molecular and Structural Biology, Jožef Stefan Institute and the Centre of Excellence for Integrated Approaches in Chemistry and Biology of Proteins, Ljubljana, Slovenia, for MALDI TOF analysis. We thank Chris Berrie for critical reading and linguistic revision of the manuscript, and Nina Orehar for excellent technical help.

Appendix A. Supplementary material

Supplementary material related to this article can be found at http://dx.doi.org/10.1016/j.biochi.2013.06.012.

References

[1] R. Cohen, L. Persky, Y. Hadar, Biotechnological applications and potential of wood-degrading mushrooms of the genus *Pleurotus*, Appl. Microbiol. Biotechnol. 58 (2002) 582–594.
[2] A.W. Bernheimer, L.S. Avigad, A cytolytic protein from the edible mushroom, *Pleurotus ostreatus*, Biochim. Biophys. Acta 585 (1979) 451–461.
[3] S. Berne, L. Lah, K. Sepčić, Aegerolysins: structure, function, and putative biological role, Protein Sci. 18 (2009) 694–706.
[4] S. Berne, I. Križaj, F. Pohleven, T. Turk, P. Maček, K. Sepčić, *Pleurotus* and *Agrocybe* hemolysins, new proteins hypothetically involved in fungal fruiting, Biochim. Biophys. Acta 1570 (2002) 153–159.
[5] S. Berne, K. Sepčić, G. Anderluh, T. Turk, P. Maček, N. Poklar Ulrih, Effect of pH on the pore forming activity and conformational stability of ostreolysin, a lipid raft-binding protein from the edible mushroom *Pleurotus ostreatus*, Biochemistry 44 (2005) 11137–11147.
[6] T. Tomita, K. Noguchi, H. Mimuro, F. Ukaji, K. Ito, N. Sugawara-Tomita, Y. Hashimoto, Pleurotolysin, a novel sphingomyelin-specific two-component cytolysin from the edible mushroom *Pleurotus ostreatus*, assembles into a transmembrane pore complex, J. Biol. Chem. 279 (2004) 26975–26982.
[7] N. Sakurai, J. Kaneko, Y. Kamio, T. Tomita, Cloning, expression, and pore-forming properties of mature and precursor forms of pleurotolysin, a sphingomyelin-specific two-component cytolysin from the edible mushroom *Pleurotus ostreatus*, Biochim. Biophys. Acta 1679 (2004) 65–73.
[8] P.H. Ngai, T.B. Ng, A hemolysin from the mushroom *Pleurotus eryngii*, Appl. Microbiol. Biotechnol. 72 (2006) 1185–1191.
[9] K. Ebina, H. Sakagami, K. Yokota, H. Kondo, Cloning and nucleotide sequence of cDNA encoding Asp-hemolysin from *Aspergillus fumigatus*, Biochim. Biophys. Acta 1219 (1994) 148–150.
[10] Y. Kudo, Y. Fukuchi, T. Kumagai, K. Ebina, K. Yokota, Oxidized low-density lipoprotein-binding specificity of Asp-hemolysin from *Aspergillus fumigatus*, Biochim. Biophys. Acta 1568 (2001) 183–188.
[11] Y. Kudo, T. Ootani, T. Kumagai, Y. Fukuchi, K. Ebin, K. Yokota, A novel oxidized low-density lipoprotein-binding protein, Asp-hemolysin, recognizes lysophosphatidylcholine, Biol. Pharm. Bull. 25 (2002) 787–790.
[12] J. Rao, A. DiGiandomenico, J. Unger, Y. Bao, R.K. Polanowska-Grabowska, J.B. Goldberg, A novel oxidized low-density lipoprotein-binding protein from *Pseudomonas aeruginosa*, Microbiology 154 (2008) 654–665.
[13] B.F. Kafsack, V.B. Carruthers, Apicomplexan perforin-like proteins, Commun. Integr. Biol. 3 (2010) 18–23.
[14] R.J. Gilbert, M. Mikelj, M. Dalla Serra, C.J. Froelich, G. Anderluh, Effects of MACPF/CDC proteins on lipid membranes, Cell Mol. Life Sci. (2012) 1–16., http://dx.doi.org/10.1007/s00018-012-1153-8.
[15] C.J. Rosado, S. Kondos, T.E. Bull, M.J. Kuiper, R.H. Law, A.M. Buckle, I. Voskoboinik, P.I. Bird, J.A. Trapani, J.C. Whisstock, M.A. Dunstone, The MACPF/CDC family of pore-forming toxins, Cell Microbiol. 10 (2008) 1765–1774.
[16] E.G. Bligh, W.J. Dyer, A rapid method of total lipid extraction and purification, Can J. Biochem. Physiol. 37 (1959) 911–917.
[17] K. Sepčić, S. Berne, C. Potrich, T. Turk, P. Maček, G. Menestrina, Interaction of ostreolysin, a cytolytic protein from the edible mushroom *Pleurotus ostreatus*, with lipid membranes and modulation by lysophospholipids, Eur. J. Biochem. 270 (2003) 1199–1210.
[18] I.V. Grigoriev, H. Nordberg, I. Shabalov, A. Aerts, M. Cantor, D. Goodstein, A. Kuo, S. Minovitsky, R. Nikitin, R.A. Ohm, R. Otillar, A. Poliakov, I. Ratnere, R. Riley, T. Smirnova, D. Rokhsar, I. Dubchak, The genome portal of the Department of Energy Joint Genome Institute, Nucleic Acids Res. 40 (2012) D26–D32.
[19] G. Anderluh, M. Beseničar, A. Kladnik, J.H. Lakey, P. Maček, Properties of nonfused liposomes immobilized on an L1 Biacore chip and their permeabilization by a eukaryotic pore-forming toxin, Anal. Biochem. 344 (2005) 43–52.
[20] G. Belmonte, C. Pederzolli, P. Maček, G. Menestrina, Pore formation by the sea anemone cytolysin equinatoxin II in red blood cells and model lipid membranes, J. Membr. Biol. 131 (1993) 11–22.
[21] O. Blixt, S. Head, T. Mondala, C. Scanlan, M.E. Huflejt, R. Alvarez, M.C. Bryan, F. Fazio, D. Calarese, J. Stevens, N. Razi, D.J. Stevens, J.J. Skehel, I. van Die, D.R. Burton, I.A. Wilson, R. Cummings, N. Bovin, C.H. Wong, J.C. Paulson, Printed covalent glycan array for ligand profiling of diverse glycan binding proteins, Proc. Natl. Acad. Sci. U. S. A 101 (2004) 17033–17038.
[22] V. Hodnik, G. Anderluh, Capture of Intact Liposomes on Biacore Sensor Chips for Protein-membrane Interaction Studies, Humana Press, 2010, pp. 201–211.
[23] M. Beseničar, P. Maček, J.H. Lakey, G. Anderluh, Surface plasmon resonance in protein–membrane interactions, Chem. Phys. Lipids 141 (2006) 169–178.
[24] G. Tang, L. Peng, P.R. Baldwin, D.S. Mann, W. Jiang, I. Rees, S.J. Ludtke, EMAN2: an extensible image processing suite for electron microscopy, J. Struct. Biol. 157 (2007) 38–46.
[25] T. Shibata, M. Kudou, Y. Hoshi, A. Kudo, N. Nanashima, K. Miyairi, Isolation and characterization of a novel two-component hemolysin, erylysin A and B, from an edible mushroom, *Pleurotus eryngii*, Toxicon 56 (2010) 1436–1442.
[26] S.H. Lee, B.G. Kim, K.J. Kim, J.S. Lee, D.W. Yun, J.H. Hahn, G.H. Kim, K.H. Lee, D.S. Suh, S.T. Kwon, C.S. Lee, Y.B. Yoo, Comparative analysis of sequences expressed during the liquid-cultured mycelia and fruit body stages of *Pleurotus ostreatus*, Fungal Genet. Biol. 35 (2002) 115–134.
[27] J.M.C. Mondego, M.F. Carazzolle, G.G.L. Costa, E.F. Formighieri, L.P. Parizzi, J. Rincones, C. Cotomacci, D.M. Carraro, A.F. Cunha, H. Carrer, R.O. Vidal,

R.C. Estrela, O. Garcia, D.P.T. Thomazella, B.V. de Oliveira, A.B.L. Pires, M.C.S. Rio, M.R.R. Araujo, M.H. de Moraes, L.A.B. Castro, K.P. Gramacho, M.S. Goncalves, J.P.M. Neto, A.G. Neto, L.V. Barbosa, M.J. Guiltinan, B.A. Bailey, L.W. Meinhardt, J.C.M. Cascardo, G.A.G. Pereira, A genome survey of *Moniliophthora perniciosa* gives new insights into Witches' Broom Disease of cacao, BMC Genomics 9 (2008) 548.

[28] R.H. Law, N. Lukoyanova, I. Voskoboinik, T.T. Caradoc-Davies, K. Baran, M.A. Dunstone, M.E. D'Angelo, E.V. Orlova, F. Coulibaly, S. Verschoor, K.A. Browne, A. Ciccone, M.J. Kuiper, P.I. Bird, J.A. Trapani, H.R. Saibil, J.C. Whisstock, The structural basis for membrane binding and pore formation by lymphocyte perforin, Nature 468 (2010) 447–451.

[29] C.J. Rosado, A.M. Buckle, R.H. Law, R.E. Butcher, W.T. Kan, C.H. Bird, K. Ung, K.A. Browne, K. Baran, T.A. Bashtannyk-Puhalovich, N.G. Faux, W. Wong, C.J. Porter, R.N. Pike, A.M. Ellisdon, M.C. Pearce, S.P. Bottomley, J. Emsley, A.I. Smith, J. Rossjohn, E.L. Hartland, I. Voskoboinik, J.A. Trapani, P.I. Bird, M.A. Dunstone, J.C. Whisstock, A common fold mediates vertebrate defense and bacterial attack, Science 317 (2007) 1548–1551.

[30] A.P. Heuck, P.C. Moe, B.B. Johnson, The cholesterol-dependent cytolysin family of Gram-positive bacteria, in: J.R. Harris (Ed.), Cholesterol Binding and Cholesterol Transport Proteins, Springer Science, 2010, pp. 551–577.

[31] E.M. Hotze, R.K. Tweten, Membrane assembly of the cholesterol-dependent cytolysin pore complex, Biochim. Biophys. Acta 1818 (2012) 1028–1038.

[32] K.J. Dowd, R.K. Tweten, The cholesterol-dependent cytolysin signature motif: a critical element in the allosteric pathway that couples membrane binding to pore assembly, PLoS Pathogens 8 (2012) e1002787.

[33] J.J. Flanagan, R.K. Tweten, A.E. Johnson, A.P. Heuck, Cholesterol exposure at the membrane surface is necessary and sufficient to trigger perfringolysin O binding, Biochemistry 48 (2009) 3977–3987.

[34] J.A.F. Opdenkamp, Lipid asymmetry in membranes, Ann. Rev. Biochem. 48 (1979) 47–71.

[35] K. Sepčić, S. Berne, K. Rebolj, U. Batista, A. Plemenitaš, M. Šentjurc, P. Maček, Ostreolysin, a pore-forming protein from the oyster mushroom, interacts specifically with membrane cholesterol-rich lipid domains, FEBS Lett. 575 (2004) 81–85.

[36] K. Rebolj, N. Ulrih-Poklar, P. Maček, K. Sepčić, Steroid structural requirements for interaction of ostreolysin, a lipid-raft binding cytolysin, with lipid monolayers and bilayers, Biochim. Biophys. Acta 1758 (2006) 1662–1670.

[37] J.R. Dankert, J.W. Shiver, A.F. Esser, Ninth component of complement: self-aggregation and interaction with lipids, Biochemistry 24 (1985) 2754–2762.

[38] J. Tschopp, E.R. Podack, H.J. Mullereberhard, The membrane attack complex of complement – C5b-8 complex as accelerator of C9 polymerization, J. Immunol. 134 (1985) 495–499.

[39] B. Westerlund, J.P. Slotte, How the molecular features of glycosphingolipids affect domain formation in fluid membranes, Biochim. Biophys. Acta 1788 (2009) 194–201.

[40] B.B. Johnson, P.C. Moe, D. Wang, K. Rossi, B.L. Trigatti, A.P. Heuck, Modifications in perfringolysin O domain 4 alter the cholesterol concentration threshold required for binding, Biochemistry 51 (2012) 3373–3382.

[41] A. Bavdek, R. Kostanjšek, V. Antonini, J.H. Lakey, M. Dalla Serra, R.J. Gilbert, G. Anderluh, pH dependence of listeriolysin O aggregation and pore-forming ability, FEBS J. 279 (2012) 126–141.

[42] G. Anderluh, J. Lakey (Eds.), Proteins: Membrane Binding and Pore Formation, Landes Bioscience, Austin, 2010.

[43] T.X. Dang, E.M. Hotze, I. Rouiller, R.K. Tweten, E.M. Wilson-Kubalek, Prepore to pore transition of a cholesterol-dependent cytolysin visualized by electron microscopy, J. Struct. Biol. 150 (2005) 100–108.

[44] S.J. Tilley, E.V. Orlova, R.J. Gilbert, P.W. Andrew, H.R. Saibil, Structural basis of pore formation by the bacterial toxin pneumolysin, Cell 121 (2005) 247–256.

[45] D.M. Czajkowsky, E.M. Hotze, Z. Shao, R.K. Tweten, Vertical collapse of a cytolysin prepore moves its transmembrane β-hairpins to the membrane, EMBO J. 23 (2004) 3206–3215.

[46] M. Lenz, S. Morlot, A. Roux, Mechanical requirements for membrane fission: common facts from various examples, FEBS Lett. 583 (2009) 3839–3846.

[47] T. Praper, A.F.P. Sonnen, A. Kladnik, A.O. Andrighetti, G. Viero, K.J. Morris, E. Volpi, L. Lunelli, M. Dalla Serra, C.J. Froelich, R.J.C. Gilbert, G. Anderluh, Perforin activity at membranes leads to invaginations and vesicle formation, Proc. Natl. Acad. Sci. U. S. A 108 (2011) 21016–21021.

[48] K. Bacia, P. Schwille, T. Kurzchalia, Sterol structure determines the separation of phases and the curvature of the liquid-ordered phase in model membranes, Proc. Natl. Acad. Sci. U. S. A 102 (2005) 3272–3277.

[49] M. Carvalho, D. Schwudke, J.L. Sampaio, W. Palm, I. Riezman, G. Dey, G.D. Gupta, S. Mayor, H. Riezman, A. Shevchenko, T.V. Kurzchalia, S. Eaton, Survival strategies of a sterol auxotroph, Development 137 (2010) 3675–3685.

[50] E.V. Entchev, T.V. Kurzchalia, Requirement of sterols in the life cycle of the nematode *Caenorhabditis elegans*, Semin. Cell Dev. Biol. 16 (2005) 175–182.

[51] K. Satouchi, K. Hirano, M. Sakaguchi, H. Takehara, F. Matsuura, Phospholipids from the free-living nematode *Caenorhabditis elegans*, Lipids 28 (1993) 837–840.

[52] P. Sperling, E. Heinz, Plant sphingolipids: structural diversity, biosynthesis, first genes and functions, Biochim. Biophys. Acta 1632 (2003) 1–15.

[53] S.C. Kondos, T. Hatfaludi, I. Voskoboinik, J.A. Trapani, R.H. Law, J.C. Whisstock, M.A. Dunstone, The structure and function of mammalian membrane-attack complex/perforin-like proteins, Tissue Antigens 76 (2010) 341–351.

Please cite this article in press as: K. Ota, et al., Membrane cholesterol and sphingomyelin, and ostreolysin A are obligatory for pore-formation by a MACPF/CDC-like pore-forming protein, pleurotolysin B, Biochimie (2013), http://dx.doi.org/10.1016/j.biochi.2013.06.012